



# Collapse mechanism of the overlying strata above a salt cavern by solution mining with double-well convection

Guimin Zhang<sup>1</sup> · Zhenshuo Wang<sup>1</sup> · Kai Zhang<sup>2</sup> · Yinping Li<sup>3</sup> · Yu Wu<sup>1</sup> · Yanlong Chen<sup>1</sup> · Houquan Zhang<sup>1</sup>

Received: 26 October 2017 / Accepted: 2 August 2018 / Published online: 22 August 2018  
© Springer-Verlag GmbH Germany, part of Springer Nature 2018

## Abstract

In solution mining of salt formations, unreasonable salt cavities formed may lead to surface collapse hazards. In this paper, a mathematical model was proposed to analyze the collapse mechanism of the overlying strata above a salt cavern induced by solution mining with double-well convection. In the proposed model, the collapses of the overlying strata were supposed to occur layer by layer, and a thin plate with four edges clamped was introduced to calculate the critical collapse span of each layer. The limit breaking distance of the thin plate can be solved by setting the corresponding surrounding condition. According to the solution, the limit breaking distance is related to the dimensions, the mechanical properties of the rock, the buried depth, and the force status. For the convenience of calculation, a span criterion was introduced to distinguish the limit breaking distance. To keep the immediate roof more stable, the span criterion should be larger. As a case study, the collapse incidents at Dongxing Salt Mine were analyzed by the proposed model, and the collapses were verified to be inevitable under its mining and geological conditions. Discussions were finally carried out to study the influences of the thickness of the immediate roof, tension strength, Poisson ratio, and buried depth on the collapses. Above all, the collapses will occur more easily with the decrease of the thickness, tension strength, and Poisson ratio of each stratum. Especially, the collapse depth will not increase linearly with the buried depth, because of the bulking effect of the overlying strata.

**Keywords** Collapse of the overlying strata · Solution mining · Double-well convection · Thin plate model · Limit breaking distance

## Introduction

Solution mining is the process of extracting soluble minerals (Johnson 1998, 2005, 2008), such as salt or potash. The method includes single-well convection and double-well convection. Thereinto, double-well convection (Fig. 1) is used widely because of its large production capacity and improvement of the recovery rate, especially in bedded salt

formations. Solution mining of bedded salt formations or salt domes typically entails creating one or several large underground cavities that are filled with brine (Shi et al. 2015). The dimensions of cavities are based largely on the thickness of the salt and the buried depth of the cavity. At some sites, the cavity becomes unreasonable, and the overlying strata above the cavity collapse unfortunately. In the USA, four well-documented collapses that resulted from solution mining are Cargill sink (Kansas), Grand Saline sink (Texas), Grosse Ile (Michigan), and Tully Valley (New York) (Johnson 2005, 2008). In France, surface subsidence above salt caverns were reported at Cerville–Buissoncourt (Karimi-Jafari et al. 2008; Contrucci et al. 2011), the SG4-5 collapse at Gellenoncourt (Buffet 1998) and the LR51 collapse at La Rape (Jeanneau 2005). In Italy, catastrophic sinkholes, with serious environmental consequences, occurred in the 1980s during salt mining in Calabria (Iovine and Parise 2008), and more recently in Piedmont (Vigna et al. 2010). Similar situations have been also registered in other European countries, as at Tuzla, Bosnia Herzegovina (Mancini

✉ Guimin Zhang  
zhangguimin08@mails.ucas.ac.cn

<sup>1</sup> State Key Laboratory for Geomechanics and Deep Underground Engineering, School of Mechanics and Civil Engineering, China University of Mining and Technology, Xuzhou 221116, Jiangsu, China  
<sup>2</sup> Geological Exploration Technology Institute of Anhui Province, Hefei 233031, Anhui, China  
<sup>3</sup> State Key Laboratory of Geomechanics and Geotechnical Engineering, Institute of Rock and Soil Mechanics, Chinese Academy of Sciences, Wuhan 430071, Hubei, China

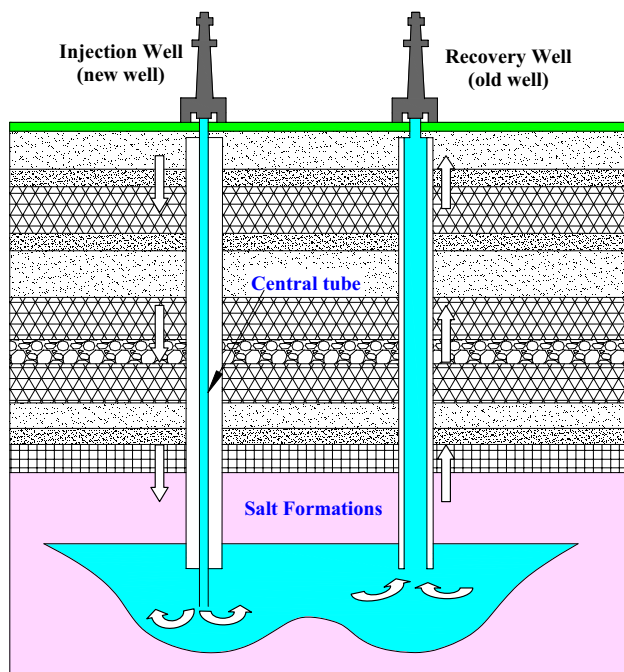


**Fig. 1** Solution mining with double-well convection

et al. 2009), and in Romania (Mesescu 2011). Surface collapse hazards induced by solution mining have happened in many places of China, such as Dongxing (Anhui) (Qiu 2011), Huichang (Jiangxi) (Long and Lin 2011), Yingcheng (Hubei) (Yu 1998a, b), and Xinli (Hunan) (Fan and Li 2008; Li et al. 2008, 2009). In these places of China, the salt formations are mostly bedded salt formations (Li et al. 2014; Zhang et al. 2014, 2015a). The surface collapse may destroy houses, roads and other infrastructures, and pollute the land and water, which has become one of the important factors affecting the safe mining of salt formations.

Surface collapse can develop within days and with little advance warning (Dahm et al. 2011; Gutierrez et al. 2014). For developing early-warning systems and/or remediation schemes from such information, it is important to understand the structural development of gravitational overburden collapses. An intrinsic problem is that this mostly occurs underground and so cannot be directly observed (Parise and Lollino 2011; Parise 2015). Consequently, many researchers have turned to analytical, analog and numerical collapse simulations. Analog models (Poppe et al. 2014; Ge and Jackson 1998) readily simulate such large discontinuous strains in a three-dimensionally complete way. Most analog modeling studies have explored the general structural geometry and kinematics of collapse. However, specific collapse dimensions and conditions still cannot be obtained or inferred because of the similarity of the analog models. Two analytical models (Bérest 2016) have been promoted to explain the creation of sinkholes above salt caverns: “piston”

model and “hour glass” model. However, it is not accurate that the collapse rocks are treated as a whole vertical cylinder and shear failure happens along the cylinder edge in the mechanical interpretation of the “piston” model, because the overlying strata or caprock should collapse layer by layer. Numerical simulation and theoretical analysis was carried out by Li et al. (2008, 2009) and Fan and Li (2008), and the stability of the immediate roof was considered to be one of the key factors to prevent the surface collapse. The ground movement law of the roof in solution mining of rock salt was studied by Liu et al. (1999), and a probability integral prediction formula for calculating subsidence anywhere in the overburden layer was deduced. Considering the sedimentary characteristics of bedded salt formations, the collapse of overlying strata and the surface subsidence would exhibit strongly stratified characteristics (Ren 2005; Ren et al. 2007), and thus a new 3D probability integral method was developed (Ren et al. 2009). However, the probability integral method was only suitable for the slow subsidence but not suitable for surface collapse accidents.

In view that the surface subsidence and collapse are related to the roof above a salt cavern, the stability of roof has been analyzed through beam model (Bauer et al. 1998; Michael and Maurice 2002; Liu et al. 2007) and circular plate model (Jiang et al. 2005; Bekendam and Paar 2002). For example, Bauer et al. (1998) studied the roof stability of long horizontal leached caverns in bedded rock salt formations and built a cantilever beam model to calculate the stresses in an interlayer. They thought shear and tensile failure were the main reasons causing roof instability. Michael and Maurice (2002) simplified the interlayer at the cavern roof as a composite beam structure to determine the minimum operating pressure, and also studied the deformation and stress of the composite beam structure. Based on the catastrophe theory and simply supported beam model, dynamic balance process and instability process of cavern roof were studied by Liu et al. (2007), and the influencing factor was also analyzed. The stability of single cavern roof was studied by Jiang et al. (2005) with cusp catastrophe model of large deformation circular plate with fixed supports. The necessary conditions of instability are deduced. Considering the level stress contributed under the weight of strata and geological construction, the cusp catastrophe of the connected well roof is analyzed with the cusp catastrophe model of beam model. Bekendam and Paar (2002) researched the mechanism of roof collapse by circular plate theory, listed several possible collapse modes, discussed the influences of brine removal on the ground subsidence, and listed several failure modes of interlayers serving as the cavern roof, such as tensile failure, shear failure, crushing rupture, and plastic yield. As a matter of fact, the circular plate model is only suitable for the salt cavities by single-well convection. Moreover,

the beam model is not so in conformity with the plate shape of the immediate roof by double-well convection.

In this paper, a new mathematical model was proposed to analyze the collapse mechanism of the overlying strata above a salt cavern induced by solution mining with double-well convection. In the model, the collapse of overlying strata was supposed to have happened layer by layer, and a thin plate with four edges clamped was introduced to calculate the critical collapse span of the current immediate roof. The limit breaking distance of the thin plate was solved by setting the corresponding surrounding condition. As a case study, the surface collapses at Dongxing Salt Mine were introduced to verify the proposed model under its mining and geological conditions. Using the proposed model, discussions were also carried out to study the influences of the thickness of the immediate roof, tension strength, Poisson ratio, and buried depth on the collapse of the overlying strata.

### Methodology

Generally, the overlying strata are sedimentary strata and deposited layer by layer. Under the action of brine and crustal stress, the current immediate roof may produce fractures and collapse during or after the solution mining. As the collapsed roof drops to the bottom of the cavity, the brine is squeezed into the upper newly formed space, and then the adjacent upper stratum becomes the immediate roof (Fig. 2). In turn, each layer of the overlying strata may become the immediate roof and ultimately collapse under the influence of brine and crustal stress. When the top stratum collapses, surface subsidence or collapse accident happens, and the brine may reach the ground surface and even form a lake (Johnson 2005, 2008; Gutiérrez et al. 2008). Therefore, it is especially necessary to propose a

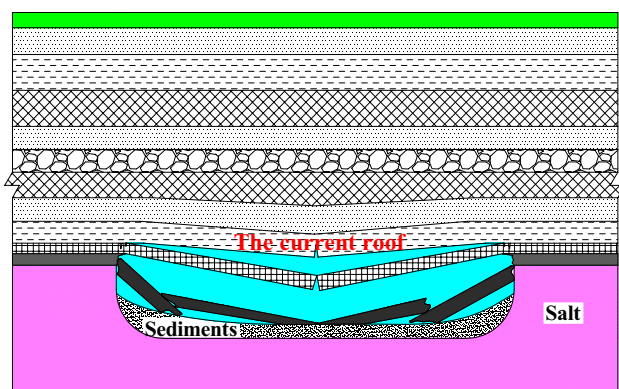


Fig. 2 Evolution of the immediate roof

mechanical model to research the collapse mechanism of the immediate roof.

### Mechanical model

For solution mining with double-well convection, the dimension of the immediate roof is determined by two mining parameters. One parameter is the solution radius of single well and the other is the well spacing between injection well and recovery well. With the progress of solution mining, the exposed area of cavern roof continues to expand. When the roof reaches a certain dimension, it starts to collapse due to lack of stability. Supposing that the collapse dimension of a specific roof is an inherent attribute, if the length of the roof is known, the limit breaking width should be calculated; if the width is known, the limit breaking length should also be calculated. In this paper, the thin plate model is introduced to calculate the limit breaking distance (length or width) for the immediate roof.

#### Thin plate model for the immediate roof

Assuming that the current immediate roof is a thin plate with four edges clamped, as shown in Fig. 3. In the figure,  $a$  indicates the length of the salt cavern, while  $b$  indicates the width. The length  $a$  and width  $b$  can be calculated as follows:

$$a = d + 2r, \tag{1}$$

$$b = 2r, \tag{2}$$

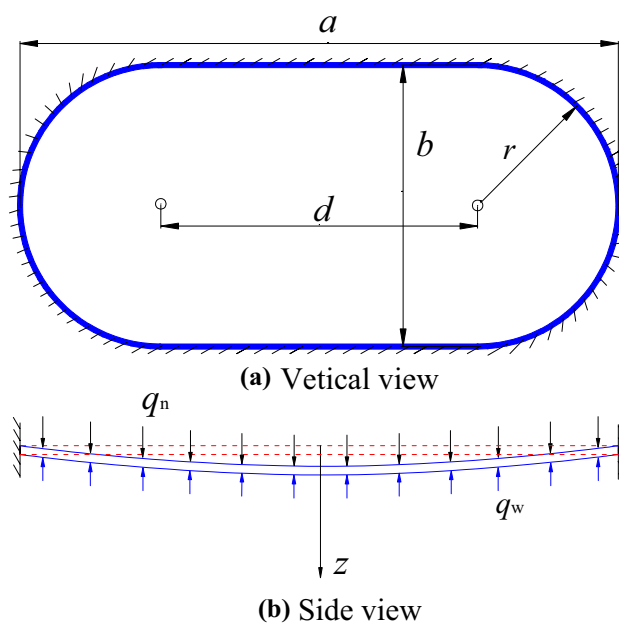


Fig. 3 Mechanical model of the cavern roof

where  $d$  is the well spacing between the injection well and the recovery well,  $m$ ; and  $r$  is the solution radius of single well,  $m$ .

In the vertical direction, the roof is affected by the uniformly distributed load  $q$ , which is the difference between the vertical crustal stress  $q_n$  and the brine pressure  $q_w$ , as shown in Fig. 3b. The vertical crustal stress  $q_n$  is caused by the overlying strata and its own gravity, and its direction is perpendicular to the horizontal plane and points to the center of the earth. The pressure of brine  $q_w$  is imposed on the bottom surface of the immediate roof, and the direction is perpendicular to the immediate roof. The uniformly distributed load  $q$  can be calculated as follows:

$$q = q_n - q_w = (\gamma_n - \gamma_w)H, \tag{3}$$

where  $\gamma_n$  indicates the average unit weight of the overlying strata,  $2.3 \times 10^3 \text{ kg/m}^3$  (Zhang et al. 2015a, b, 2017);  $\gamma_w$  indicates the unit weight of the brine,  $1.2 \times 10^3 \text{ kg/m}^3$  (Zhang et al. 2015b); and  $H$  indicates the buried depth of the current immediate roof,  $m$ .

In particular, Eq. (3) is based on the following condition: the cavity is full when the collapse of immediate roof occurs. Undeniably, there may be other situations. For example, as the immediate roof collapses, the brine enters in the newly formed fissures, pores or holes, which may induce the cavity to be not completely filled. As a result, voids may develop between the current roof and brine. Under this condition, the bottom of the current roof will lack the support of brine, namely the  $q_w$  in Eq. (3) no longer exists. In short, Eq. (3) cannot summarize the collapse of immediate roof without brine support. However, if the current roof is shallow enough, the groundwater may flow into the upward cavity and mix with the brine, and then Eq. (3) becomes valid again. According to the site record (Qiu 2011), during the collapse process of Dingyuan Salt Mine, a column of brine came out from the wellhead. The column was primarily a few meters in height and slowly decreased with time until it was difficult to be observed. This indirectly explains that the brine was always filled inside the cavity during the surface collapses of Dingyuan Salt Mine, namely brine pressure ( $q_w$ ) was not equal to zero. Therefore, Eq. (3) meets the situation of Dingyuan Salt Mine and can be used to solve the collapse problems at Dingyuan and similar cases, such as Hutchinson, Kansas (Waltham et al. 2005) and Wink Sink 1#, Texas (Johnson 2008).

### Solution of the thin plate model

According to Marcus reduction algorithm (Qian et al. 2010), a thin plate with four edges clamped can be divided into a series of beams. In the center, the plate is treated as the cross beams. When the immediate roof is at the limit suspended state, the bending moment is negative at the four clamped

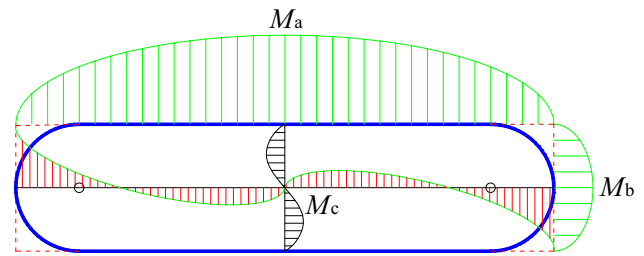


Fig. 4 Bending moment of the immediate roof with four edges clamped

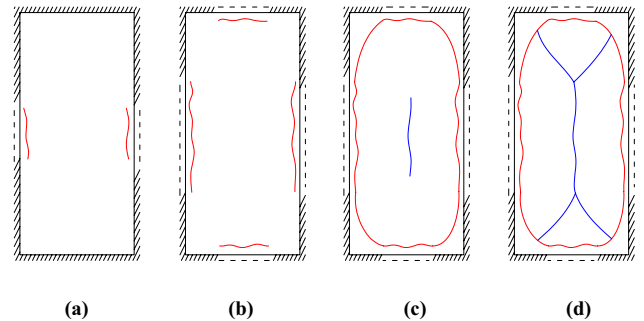


Fig. 5 “O–X” failure mode of the immediate roof (the red lines indicate the fractures at the top of the roof, while the blue ones are at the bottom)

edges and positive at the center of the plate (Fig. 4). The maximum negative bending moment ( $M_a$ ) is at the center of the long side, while the maximum positive ( $M_c$ ) is at the center of the plate.

The values of  $M_a$  and  $M_c$  can be calculated according to the Marcus modified solution:

$$M_a = -\frac{(1 - \mu^2)[1 + \mu(b/a)^2]}{12[1 + (b/a)^4]} \times qb^2, \tag{4}$$

$$M_c = -\frac{(1 - \mu^2)\left(\frac{b}{a}\right)^2 [\mu + \mu^2]}{12\left[1 + \left(\frac{b}{a}\right)^4\right]} \times qa^2, \tag{5}$$

where  $\mu$  is the Poisson ratio.

For sedimentary rock, the tension strength is generally 1/4–1/25 times as much as the uniaxial compressive strength, with an average of 1/10 (Cai et al. 2002). In view that the tension strength of sedimentary rock is very low, it is necessary to avoid it from experiencing tension stress. Once the rock reaches its tension strength, the failure will occur. According to the thin plate theory, the maximum value of the absolute value of the bending moment locates at the midpoint of the upper long edges, and thus tensile fractures will

first occur here (Fig. 5a). Then tensile fractures will occur at the midpoint of the upper short sides (Fig. 5b). Once the upper fractures link to each other and form an “O” shape, the bending moment at the center of the plate’s bottom reaches the maximum (Fig. 5c). The tension stress at the plate’s bottom may exceed the tension strength. Then cracks will generate gradually, link to each other, and finally form an “X” shape failure zones, as shown in Fig. 5d. Moreover, the profile of the tensile cracks at the top looks like a “V,” while that at the bottom looks like a “Λ”. In China, it is famously known as “O–X fracture” and verified by site observation and model material tests of coal roof by longwall mining (Wang and Qian 1989; Qian and He 1991; Qian and Xu 1998; Qian et al. 2010; Liu et al. 2015). In the collapse cases of Dingyuan Salt Mine, the shape and force characteristics of the immediate roof formed by solution mining with double-well convection are similar to the coal roof by longwall mining, so the “O–X fracture” is introduced to analyze the Dingyuan collapse hazards.

According to the maximum tensile stress strength criterion (Eq. 6), local tensile failure will happen, if the absolute value of maximum principal stress  $\sigma_1$  reaches tension strength  $\sigma_t$ .

$$\sigma_1 = \sigma_t, \tag{6}$$

where  $\sigma_1$  indicates the maximum principal stress, MPa; and  $\sigma_t$  indicates the tension strength, MPa.

As to a beam with unit width in the immediate roof, local tensile failure will occur if the bending moment  $M_a$  reaches the tension strength, as shown in the following equation:

$$M_a = \frac{h^2 \sigma_t}{6}, \tag{7}$$

where  $h$  indicates the thickness of the immediate roof, m.

Substituting Eq. (7) into Eq. (4), a relationship between the width ( $b$ ) and length ( $a$ ) can be obtained when the roof is suffered from local tensile failure. As mentioned above, if the length of the roof is known, a limit breaking width of the roof can be calculated. In this paper, the width of the roof ( $b$ ) is defined as the limit breaking distance ( $\bar{b}$ ). It can be obtained from the following equation:

$$\bar{b} = \frac{h}{1 - \mu^2} \sqrt{\frac{2\sigma_t}{q} \cdot \frac{1 + \left(\frac{\bar{b}}{a}\right)^4}{1 + \mu\left(\frac{\bar{b}}{a}\right)^2}}. \tag{8}$$

According to Eq. (8), the limit breaking distance of the thin plate is related to the dimensions (the length  $a$  and the thickness  $h$ ), the mechanical properties of the rock (the tension strength  $\sigma_t$  and the Poisson ratio  $\mu$ ), the buried depth ( $H$ , which affects the distributed load  $q$ ) and the force status (the

distributed load  $q$ ). In addition, a span criterion  $l_m$  is introduced as Eq. (9). Especially, when  $a \rightarrow \infty$ , the limit breaking distance  $\bar{b}$  is equal to the span criterion  $l_m$ . Namely,  $l_m$  is the limit distance of infinite strip with four sides clamped:

$$l_m = \frac{h}{1 - \mu^2} \sqrt{\frac{2\sigma_t}{q}}, \tag{9}$$

where  $l_m$  is the span criterion of the limit breaking distance, which is only related to the properties ( $\sigma_t$ ,  $h$ ,  $\mu$  and  $q$ ) of the immediate roof, m.

Correspondingly, a new symbol  $\omega$  is introduced to represent the remaining part of the limit breaking distance  $\bar{b}$ , shown as follows:

$$\omega = \sqrt{\frac{1 + \left(\frac{\bar{b}}{a}\right)^4}{1 + \mu\left(\frac{\bar{b}}{a}\right)^2}}. \tag{10}$$

For the convenience of calculation, the limit breaking distance  $\bar{b}$  can be obtained as follows, where  $\mu\left(\frac{\bar{b}}{a}\right)^2$  is ignored.

$$\bar{b} = \begin{cases} a^4 \sqrt{\frac{l_m^2}{a^2 - l_m^2}} & (l_m < a < \sqrt{2}l_m) \\ \frac{a}{\sqrt{2}l_m} \sqrt{a^2 - \sqrt{a^4 - 4l_m^4}} & (a \geq \sqrt{2}l_m) \end{cases}. \tag{11}$$

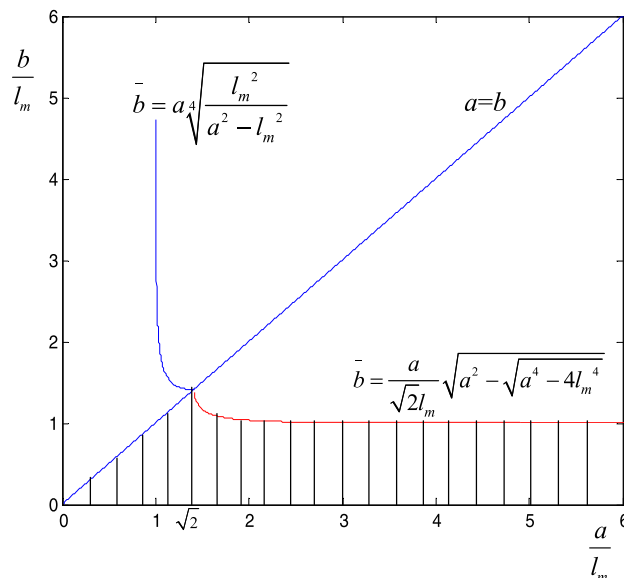


Fig. 6 The changing trend of limit breaking distance  $\bar{b}$  along with the length  $a$

Equation (11) can be figured out using the mathematical software MATLAB, as shown in Fig. 6. In the figure, the shaded region figures out the necessary condition for a roof to remain stable. Some laws can also be obtained as follows:

1. if  $\frac{a}{l_m} > \sqrt{2}$ , the limit breaking distance  $\bar{b}$  will be tending to the span criterion  $l_m$ . Under this condition, as long as the cavern width  $b$  is less than limit breaking distance  $\bar{b}$ , the roof will remain stable. In view that the cavern width  $b$  is smaller than length  $a$ , the condition in which the immediate roof keeps stable is as follows:

$$b < \bar{b} = \frac{a}{\sqrt{2}l_m} \sqrt{a^2 - \sqrt{a^4 - 4l_m^4}}, \text{ and } \frac{a}{l_m} > \sqrt{2}; \tag{12}$$

2. if  $\frac{a}{l_m} = \frac{\bar{b}}{l_m} = \sqrt{2}$ , the length  $a$  is equal to the width  $b$ , namely the well spacing  $d$  is zero. As a matter of fact, this condition belongs to the single-well convection, and the shape of roof is not a rectangle but a circle. The condition in which the roof does not break is as follows:

$$b < \bar{b} = a = \sqrt{2}l_m; \tag{13}$$

3. if  $\frac{a}{l_m} < \sqrt{2}$ , then  $\frac{\bar{b}}{l_m} > \sqrt{2}$ . Under this condition, the limit breaking distance  $\bar{b}$  is larger than the cavern length  $a$ . Because the width  $b$  is throughout no more than the length  $a$ , the cavern roof will remain stable and does not break.

Based on the above analysis, the whole limit breaking condition for the roof to keep stable can be calculated as Eqs. (12 and 13). It can be easily inferred that the bigger the length  $a$  is, the easier the stratum will collapse. From Eq. (1), the length  $a$  is the sum of the solution radius  $r$  and the well spacing  $d$ , and the width  $b$  is two times of the radius  $r$ . Because the solution radius  $r$  is believed to be a constant (40 m) due to the limitation of technical level in China, the length of the roof  $a$  is related to the well spacing  $d$  linearly, while the width  $b$  can be regarded as a constant. Therefore, to keep the roof stable, the well spacing between the injection well and the recovery well  $d$  should not be larger than the threshold value inferred from the above equations.

In addition, the limit breaking distance ( $\bar{b}$ ) is in direct proportion to the span criterion  $l_m$  from Eqs. (8) and (9). To keep the immediate roof more stable, the limit breaking distance ( $\bar{b}$ ) should be larger, namely the span criterion  $l_m$  should be larger.

### Mechanical properties of the overlying strata

To apply the above mechanical model, the geological and mechanical properties (the thickness  $h$ , the depth  $H$ , the Poisson ratio  $\mu$ , and the tension strength  $\sigma_t$ ) should be obtained in advance. Respectively, the thickness  $h$  and the depth  $H$  can be obtained from the drilling data, the Poisson ratio  $\mu$  can be obtained by uniaxial compressive tests, and the tension strength  $\sigma_t$  can be got by Brazilian splitting tests.

The uniaxial compressive and Brazilian splitting tests should comply with the ISRM-suggested methods for rock characterization, testing and monitoring (Ulusay 2014). According to the suggested methods, five samples are needed for each test. To ensure the similarity of the rock samples as much as possible, samples with almost the same content of impurity and without cracks need to be selected. Under uniaxial compressive test,  $\mu$  is a constant in the elastic deformation phase and can be calculated as follows:

$$\mu = \left| \frac{\epsilon_3}{\epsilon_1} \right|, \tag{14}$$

where  $\epsilon_1$  is the axial strain;  $\epsilon_3$  is the radial strain.

In Brazilian splitting test, a concentrated load is applied along the diameter of the specimen, and the specimen may be cracked along the diameter direction. The formula for determining the tensile strength of rock is as follows (Cai et al. 2002):

$$\sigma_t = \frac{2P}{\pi DL}, \tag{15}$$

where  $\sigma_t$  indicates the tensile strength of rock, MPa;  $P$  is the maximum force applied on the specimen when the splitting failure occurs, N;  $D$  is the diameter of the rock specimen, m;  $L$  is the thickness of the specimen, m.

### Overall view of the research

In the following text, three surface collapses at Dongxing Salt Mine are introduced as a case study to verify the proposed model. First, some necessary conditions are presented, including the geology and mining method, the detailed collapsed process and related geophysical survey. Second, the limit breaking distance  $\bar{b}$  and the span criterion  $l_m$  for each layer of the overlying strata will be calculated by the proposed model to analyze the collapse incidents. Finally, discussions will be also carried out to study the influences of the thickness of the immediate roof, tension strength, Poisson ratio, and buried depth on the collapse of the overlying strata.

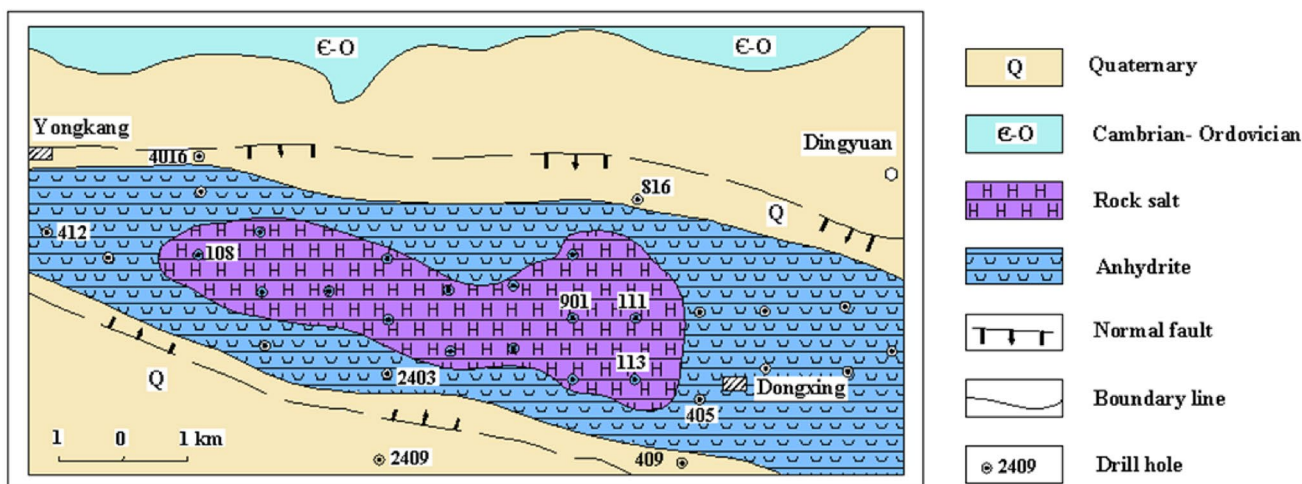
### Dongxing salt mine

#### Location, geology and mining method

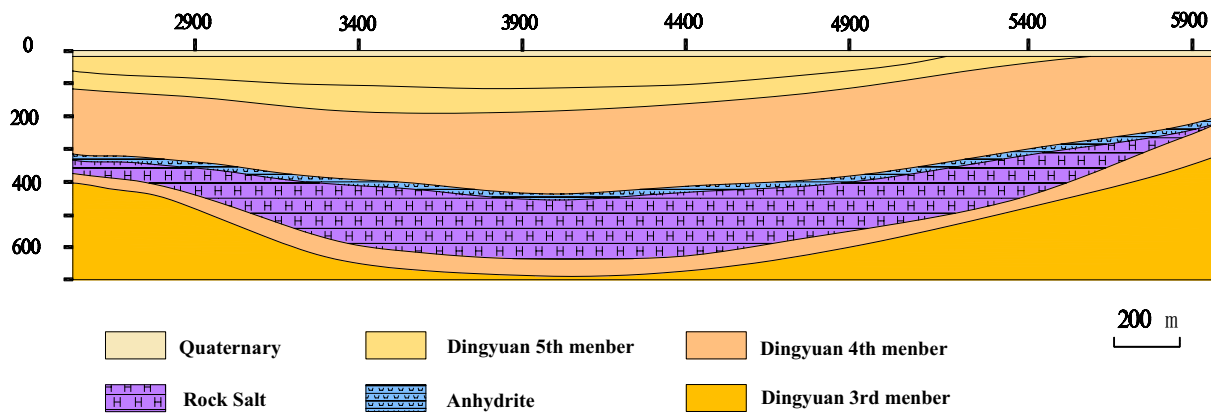
Rich resources of rock salt and Glauber’s salt are buried in the underground of Dingyuan County, China. China Salt Dongxing Salt Chemical Co., Ltd (CNSIC) is one of the biggest salt miners in Dingyuan, which is located at the Dingyuan-Luqiao sub-depression. The geologic ages of strata distributed are mainly Cenozoic Eogene System (E) and Quaternary System (Q). The north and south sides of the basin are both EW faults. Dongxing Salt Mine is located at the graben structure formed, as shown in Fig. 7. From the geological ichnography of Dingyuan Salt Mine, the overlying strata of the mining area should be intact, although there may be some primary cracks. The whole

shape of ore bodies is an irregular oval, whose long axial direction strikes from east to west with a length of about 8500 m and a width of about 2390 m, as shown in Fig. 7a. The total area reaches about 14.4 km<sup>2</sup>. The widely distributed outcropping stratum belongs to Qiju Group of Late Pleistocene Series (Qp3q). The lithologies of Qp3q are mainly silty clay and sandy clay, with an average thickness of about 20–30 m. Below the Qp3q is the thick Eogene Tujinshan Group (E<sub>2</sub>t). The main lithologies of E<sub>2</sub>t are sandstone, mudstone, salt formations and gypsum mudstone, with a total thickness up to 1100 m, as shown in Figs. 7b and 8.

According to Fig. 7b, the sedimentary region of rock salts is a basin or trough. The buried depth is deep at the middle, while the side is shallow. In the whole basin, the rock salts are buried continuously at depth 300–600 m. The total thickness is generally 60–160 m and the maximum thickness is up



(a) Geological scheme of rock salt in horizontal direction



(b) Geological cross section (unit m)

Fig. 7 Geological sketch of rock salt in Dingyuan Salt Mine

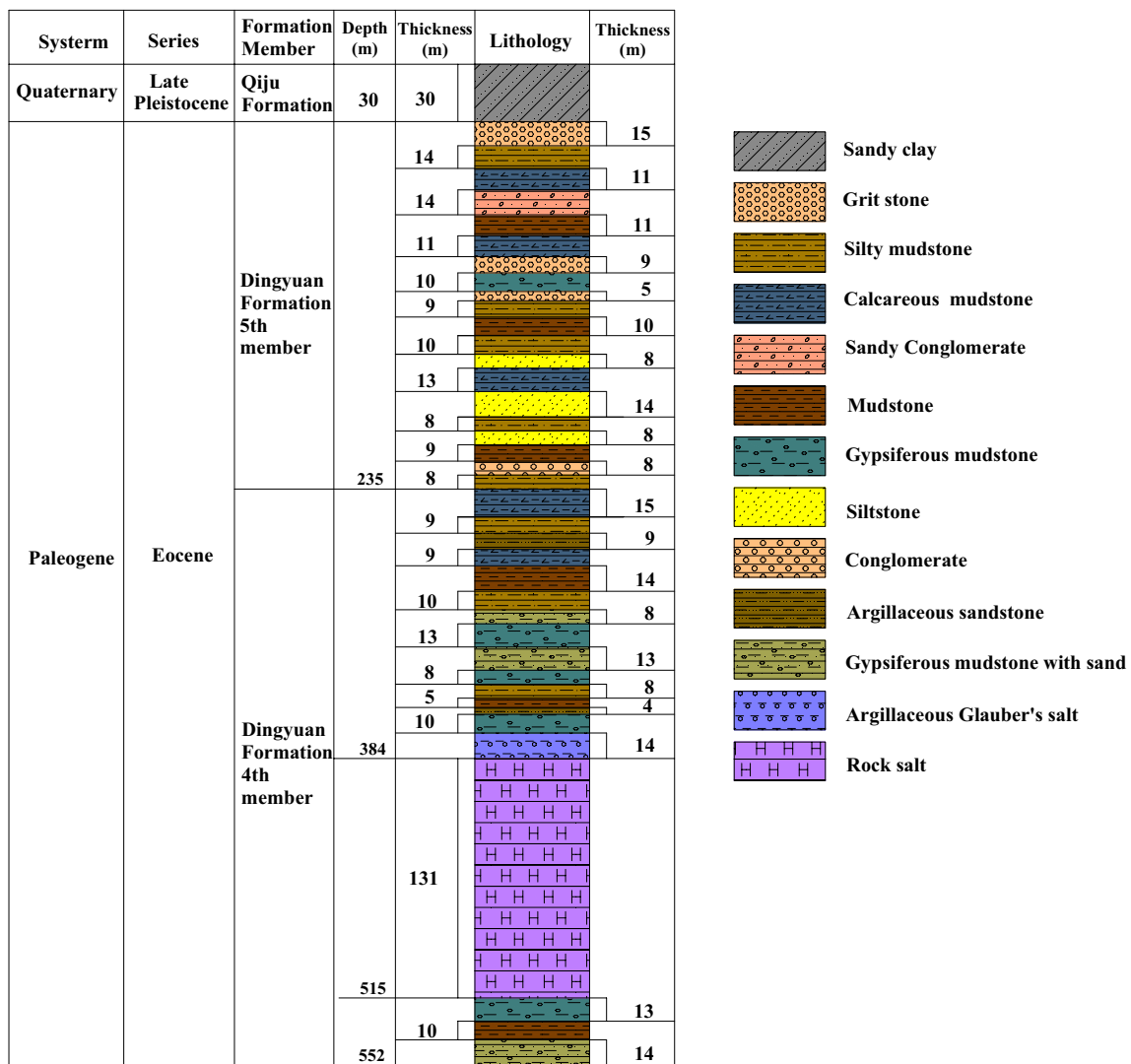


Fig. 8 Stratigraphic column of Dongxing Salt Mine

to 200 m at the center of the basin. Generally, the thickness of a single salt layer is 1–5 m and the thickest (at the middle of the basin) is about 10 m.

The mining of Dongxing Salt Mine lasted for 30 years. The original mining method was the single-well convection. Because of low recovery rate and low production capacity, the single-well convection has more and more limitations. To improve the efficiency of mining, solution mining with double-well convection was adopted to replace the single-well convection.

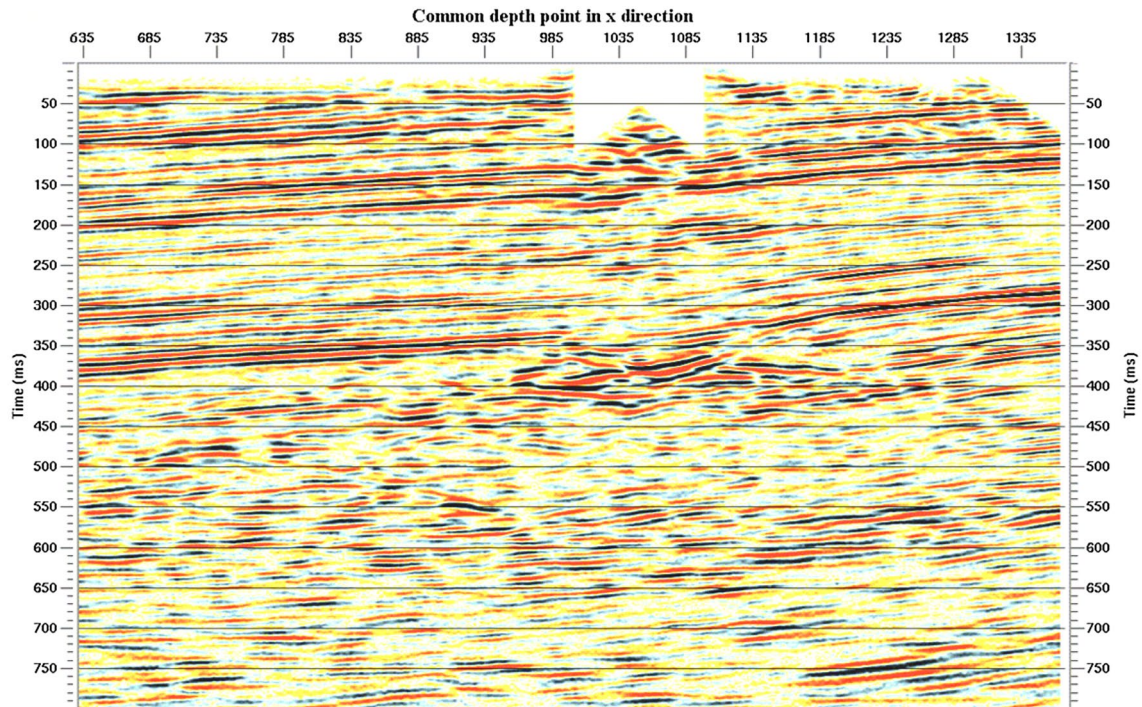
### The three collapse incidents

On 10 April 2012, the third collapse sinkhole happened at Dongxing Salt Mine (Zhang et al. 2015c), following the first one which occurred on 14 December 2005, and the second one that took place on 25 March 2006 (Zhang and Wang

2010). Three mining wells (#7, #34 and #8) fell into the sinkhole in the first collapse, while, respectively, two mining wells (#3 and #24 in the second one, #z1 and #x1 in the third one) fell into each of the other two sinkholes. The three collapse sinkholes in Dongxing Salt Mine are hazards induced by human activities. The outline of the first sinkhole in the overlying strata is shown in Fig. 9. From the figure, the collapsed body is almost a vertical cylinder, and the collapses wall is steep.

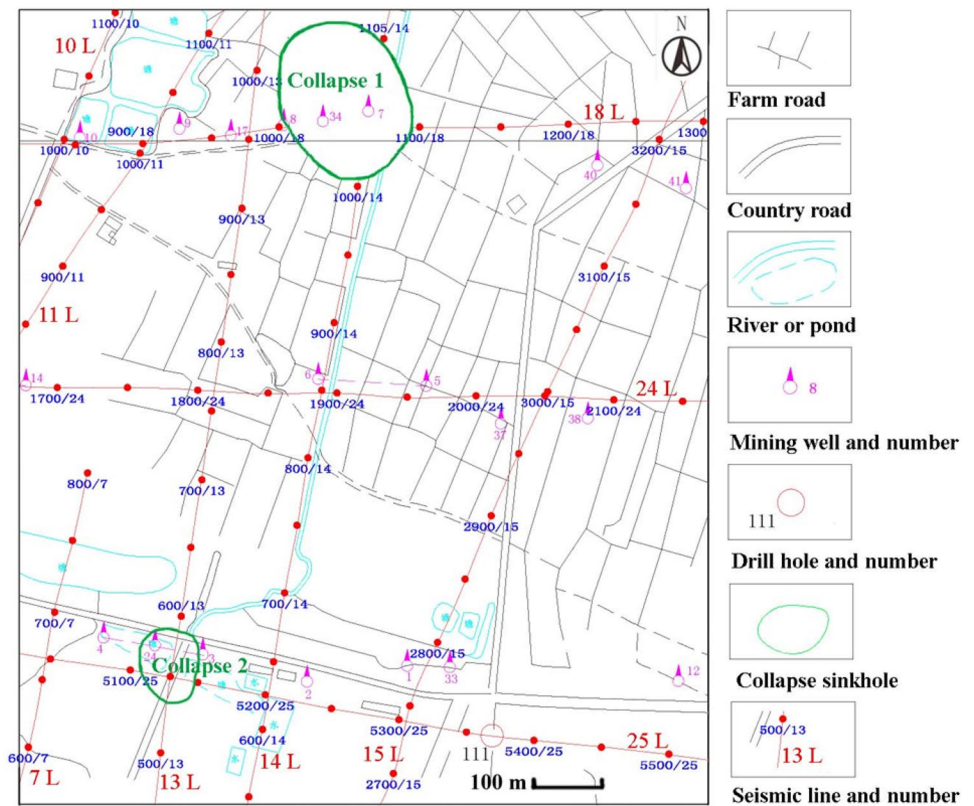
In fact, immediately after the first collapse, geophysical explorations were carried out by the Geological Exploration Technology Institute of Anhui Province to provide temporary safety forecasts for the nearby villagers (Zhang and Wang 2010). The high-density resistivity method was first used to detect whether there was a cavity in the underground within – 100 m at the whole salt mine. Second, the integrity of the anhydrite roof was used to identify whether





**Fig. 9** The outline of the first sinkhole in the overlying strata (Modified from Zhang and Wang 2010, 2015c)

**Fig. 10** Distribution of the seismic line by the four-dimensional seismic exploration (Modified from Zhang and Wang 2010, 2015c)



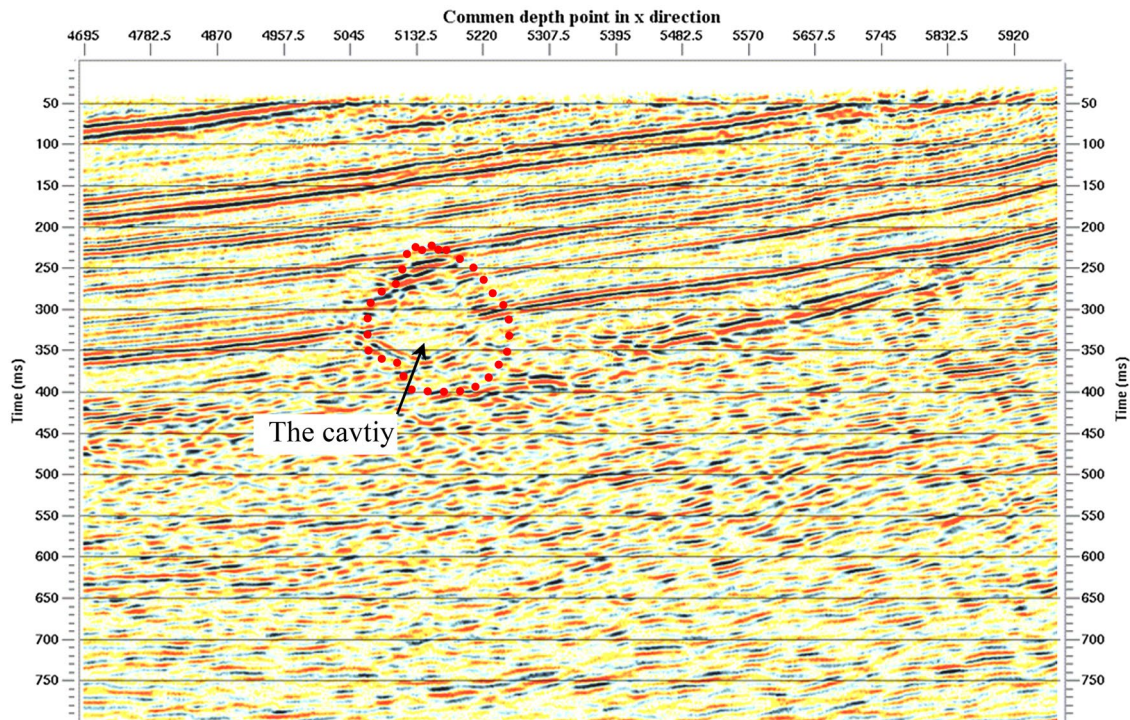


**Fig. 11** Seismic exploration result of the second sinkhole (from 25 L) (Modified from Zhang et al. 2015c)

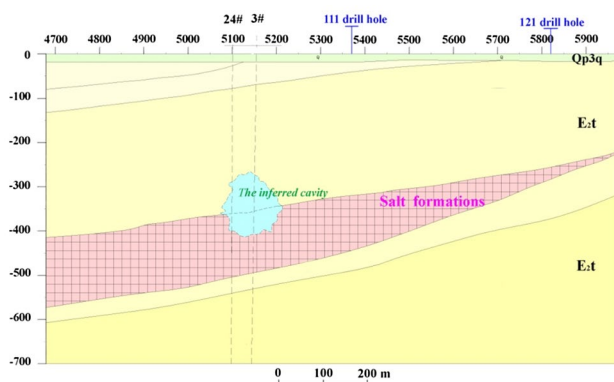


**Fig. 12** Result interpretation of the second sinkhole

there could be a risk of collapse or not. Once the anhydrite roof is destroyed, the cavity may reach a larger scale, and the possibility of failures will increase. Third, the four-dimensional seismic exploration (3D + time) was further carried out to monitor whether the cavities are abnormal or not in the entire mining area (Fig. 10). If a cavity develops continuously upward, the implemented “+” or “#” monitoring should be carried out to track its development.

Through the analysis of the seismic exploration data, an abnormal cavity (Figs. 11, 12) was found on 12 January 2006. Then, an extensive tracking and monitoring

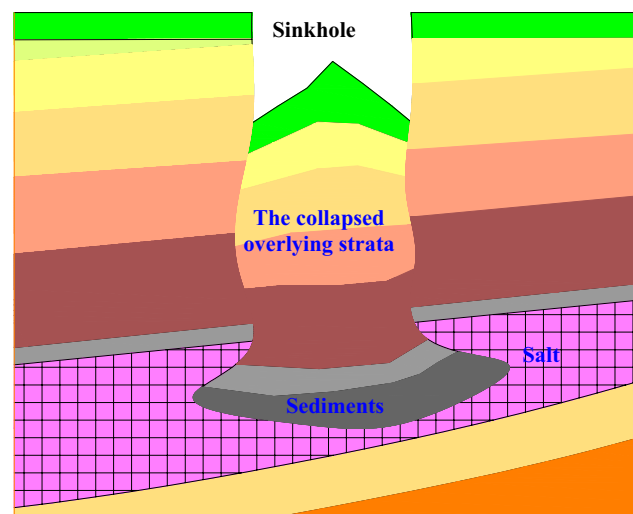


**Fig. 13** Collapse of the overlying strata layer by layer

was implemented, and after 73 days the second collapse occurred. Another abnormal cavity was found on November 2011 (Zhang et al. 2015c). After 97 days’ tracking and monitoring, the third collapse happened at 14:00 on 10 April 2012. According to the tracking and monitoring data, the whole collapse was inferred to have happened step by step, namely the overlying strata should be dropped down layer by layer (Fig. 13).

## Results and discussion

### Collapse analysis of Dongxing Salt Mine

In Dongxing Salt Mine, the thickness of each stratum above salt formations is generally 4–15 m (Fig. 8). In view of the technical level of solution mining in China, the maximum solution radius is 40 m for a single well. Supposing that the solution radius  $r$  is 40 m, the width of the immediate roof will be a constant 80 m. In addition, the length of the immediate roof is approximately 120–340 m by double-well convection. For each overlying stratum, the ratio of the thickness and the width lies mostly between 1/5–1/20. Therefore, no matter which one of the overlying strata becomes the current immediate roof, it can be seen as a thin plate with four edges clamped.

According to Eqs. (8) and (9), to keep an overlying stratum more stable, the span criterion  $l_m$  should be larger. In other words, the smaller the span criterion  $l_m$ , the worse the stability of the immediate roof. To calculate the span criterion  $l_m$ , the thickness  $h$  and the depth  $H$ , the Poisson ratio  $\mu$ , and the tension strength  $\sigma_t$  were obtained from the previous geological and mechanical data (Fig. 14) by the China Salt Dongxing Salt Chemical Co., Ltd (CNSIC) and the Geological Exploration Technology Institute of Anhui Province (Zhang and Wang 2010, 2015c).

Table 1 lists the calculated collapse parameters, akin to the span criterion  $l_m$ , the ratio  $\frac{a}{l_m}$  and the limit breaking distance  $\bar{b}$ . If the finally calculated limit breaking distance  $\bar{b}$  is lower than the width of the immediate roof (80 m), the immediate roof can be believed to be collapsed inevitably. From Table 1, most of the limit breaking distances of the overlying stratum are far shorter than 80 m, except the upper

grit stone and sandy Conglomerate in Member 5 of Dingyuan Formation. It means that most of the overlying stratum will be collapsed according to the proposed model when they are exposed as the immediate roof. However, the above analysis is based on the knowledge that the mechanical parameters of the strata are constant. As a matter of fact, the mechanical parameters of the rock will become weaker and weaker under the action of brine, which will finally result in the instability of the roof. In addition, there may be some primary fractures in the stratum. These primary fractures may also result in the instability of the roof. However, the exact distributions and dimensions of these fractures are difficult to be obtained, and then the weakness effect of the primary fractures on the strata is also difficult to quantify at present. So the influence of the primary fractures was not considered in the present study. The weakness of the above two strata under the immersion of brine will be explained in the following text.

As a special case, the upper grit stone has the biggest the span criterion  $l_m$ , which is up to 119.03. Correspondingly, the ratio  $\frac{a}{l_m}$  lies in the range  $\frac{a}{l_m} < \sqrt{2}$ . Under this condition, the limit breaking distance  $\bar{b}$  is far larger than the cavern length ( $a$ ). In view that the width  $b$  is throughout less than the length  $a$ , the limit breaking distance  $\bar{b}$  is certainly larger than the cavern width ( $b$ ). According to the above analysis, the upper grit stone will remain stable when it is exposed as the cavern roof. In addition, the limit breaking distance  $\bar{b}$  of the sandy Conglomerate is equal to 96.39, which is also larger than the width of the salt cavern. It means that the sandy Conglomerate will also remain stable and does not collapse under normal circumstances.

Actually, all of the overlying strata were collapsed in the three incidents, including both the upper grit stone and the sandy Conglomerate in Member 5 of Dingyuan Formation. The reason may be that the mechanical properties of the above two strata became weaker and weaker under the immersion of the brine. Generally, the saturation brine is only saturated with halite (NaCl). As regards the other soluble salt, they can still be dissolved in halite-saturated brine. Therefore, under the immersion of brine, the soluble components in the immediate roof are first dissolved. After a long time of immersion in brine, the strong stratum will become weaker and weaker. Finally, the overall structure of the stratum will lose its integrity and lead to its collapse inevitably. According to the above analysis, the immersion of brine will introduce huge impact on the adjacent strata, especially on those directly above the cavity. Therefore, certain salt formations above salt cavity should not be mined in engineering practice. As a protection, this layer can be used for preventing upward movement of brine.

To analyze when the grit stone will produce tensile crack under the immersion of brine, the tension strength

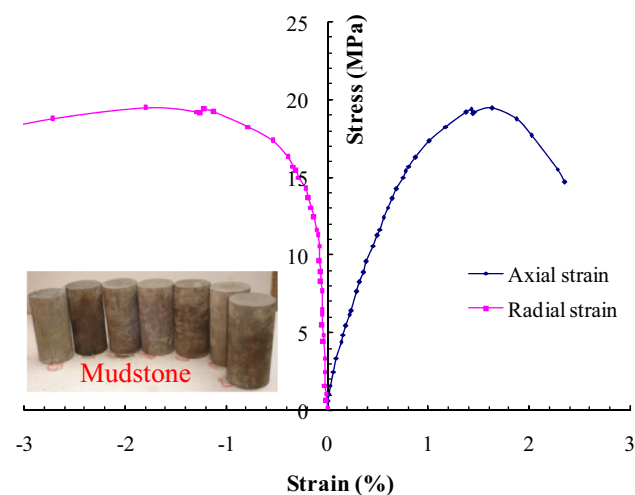


Fig. 14 Typical stress–strain curve under the uniaxial compressive test

**Table 1** Geological and mechanical parameters of the overlying strata and the calculated collapse parameters

	Lithology	$H$ (m)	$h$ (m)	$\sigma_t$ (MPa)	$\mu$	$l_m$ (m)	$\frac{a}{l_m}$	$\bar{b}$ (m)
1	Sandy clay	15.0	30	0.10	0.27	35.63	3.37	35.77
2	Grit stone	37.5	15	10.00	0.35	119.03	1.01	/
3	Silty mudstone	52.0	14	5.00	0.30	64.33	1.87	67.47
4	Calcareous mudstone	64.5	11	6.00	0.27	48.80	2.46	49.50
5	Sandy conglomerate	77.0	14	10.00	0.40	80.99	1.48	96.39
6	Mudstone	89.5	11	2.00	0.25	23.65	5.07	23.67
7	Calcareous mudstone	100.5	11	6.00	0.27	39.09	3.07	39.32
8	Grit stone	110.5	9	10.00	0.35	41.60	2.88	41.92
9	Gypsiferous mudstone	120.0	10	4.00	0.29	26.88	4.46	26.92
10	Grit stone	127.5	5	10.00	0.35	21.52	5.58	21.53
11	Silty mudstone	134.5	9	5.00	0.30	25.71	4.67	25.74
12	Mudstone	144.0	10	2.00	0.25	16.95	7.08	16.96
13	Silty mudstone	154.0	10	5.00	0.30	26.70	4.49	26.74
14	Siltstone	163.0	8	8.00	0.32	26.62	4.51	26.66
15	Silty mudstone	173.5	13	5.00	0.30	32.70	3.67	32.80
16	Siltstone	187.0	14	8.00	0.32	43.50	2.76	43.89
17	Mudstone	198.0	8	2.00	0.25	11.56	10.38	11.57
18	Siltstone	206.0	8	8.00	0.32	23.68	5.07	23.70
19	Mudstone	214.5	9	2.00	0.25	12.50	9.60	12.50
20	Grit stone	223.0	8	10.00	0.35	26.03	4.61	26.06
21	Silty mudstone	231.0	8	5.00	0.30	17.44	6.88	17.45
22	Calcareous mudstone	242.5	15	6.00	0.27	34.32	3.50	34.44
23	Silty mudstone	254.5	9	5.00	0.30	18.69	6.42	18.70
24	Argillaceous sandstone	263.5	9	6	0.28	19.87	6.04	19.88
25	Calcareous mudstone	272.5	9	6.00	0.27	19.42	6.18	19.43
26	Mudstone	284.0	14	2.00	0.25	16.90	7.10	16.90
27	Silty mudstone	296.0	10	5.00	0.30	19.26	6.23	19.27
28	Sandy conglomerate	305.0	8	10.00	0.40	23.25	5.16	23.27
29	Gypsiferous mudstone	315.5	13	4.00	0.29	21.55	5.57	21.56
30	Gypsiferous mudstone with sand	328.5	13	6.00	0.31	26.21	4.58	26.24
31	Gypsiferous mudstone	339.0	8	4.00	0.29	12.79	9.38	12.80
32	Silty mudstone	347.0	8	5.00	0.30	14.23	8.43	14.23
33	Mudstone	353.5	5	2.00	0.25	5.41	22.18	5.41
34	Argillaceous sandstone	358.0	4	6	0.28	7.58	15.84	7.58
35	Gypsiferous mudstone	365.0	10	4.00	0.29	15.41	7.79	15.42
36	Argillaceous Glauber's salt	377.0	14	6	0.34	26.93	4.46	26.97

was supposed to be gradually decreased from 10 to 1 MPa. With all other parameters as in Table 1, the influence of tension strength  $\sigma_t$  on the span criterion  $l_m$  was analyzed. Substituting the specific values of the tension strength into Eq. 9, a curve (Fig. 15) can be drawn about the influence of the tension strength  $\sigma_t$  on the dimensionless number  $l_m$ . As shown in Fig. 15, the span criterion  $l_m$  decreases gradually from 119.03 to 37.64 m, as the tension strength  $\sigma_t$  decreases.

The influence of tension strength  $\sigma_t$  on the limit breaking distance  $\bar{b}$  is shown in Table 2. From the table, the limit breaking distance  $\bar{b}$  decreases with the decrease of the tension strength  $\sigma_t$ . Especially, when the tension strength  $\sigma_t$  is equal to 4.0 MPa, the limit breaking distance  $\bar{b}$  reaches 83.74 m. That

is, the immediate roof will produce tension fracture and finally collapse. Above all, the weakness of tension strength  $\sigma_t$  will finally result in the collapse of the strong stratum.

According to the above analysis, under the double-well convection, the surface collapse of Dongxing Salt Mine is inevitable because of its specific geological condition and the immersion of brine.

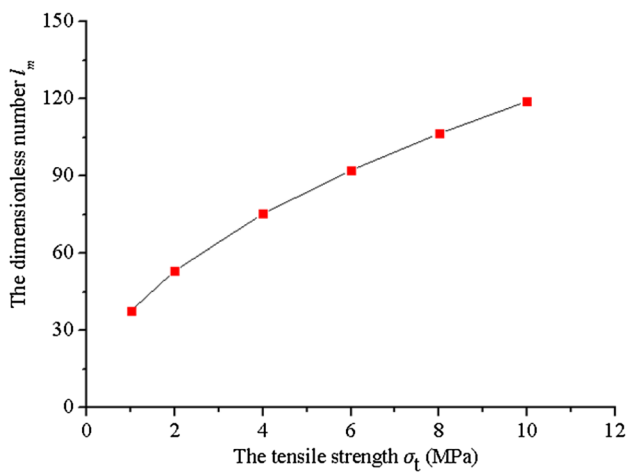


**Fig. 15** Influence of the tension strength  $\sigma_t$  on the dimensionless number  $l_m$

**Table 2** Influence of tension strength on the limit breaking distance

	Tension strength $\sigma_t$ (MPa)	Dimensionless number $l_m$ (m)	Ratio $\frac{\sigma}{l_m}$	Limit breaking distance $\bar{b}$ (m)
1	10.00	119.03	1.01	/
2	8.00	106.46	1.13	/
3	6.00	92.20	1.30	/
4	4.00	75.28	1.59	83.74
5	2.00	53.23	2.25	54.35
6	1.00	37.64	3.19	37.83

## Discussion

### The span criterion $l_m$

From the proposed model, the collapse of the immediate roof is related to the span criterion  $l_m$ . To keep the immediate roof more stable, its span criterion  $l_m$  should be larger. Especially, some important conclusions and meaningful suggestions inferred from Eq. 9 are drawn as follows:

1. The span criterion  $l_m$  is linear to the thickness  $h$  of the immediate roof. In detail, if the immediate roof is thicker, the span criterion  $l_m$  will be bigger, which means that the collapse of the roof will be harder. In other words, if there are many thin layers in the overlying strata, the surface collapse would occur much easily. Therefore, reasonable position of the solution mining should be selected to avoid the presence of many thin layers directly above the cavity.
2. The span criterion  $l_m$  is in direct proportion to the square root of the tension strength  $\sigma_t$ . If the tension strength  $\sigma_t$

of the immediate roof is higher, the span criterion  $l_m$  will be bigger correspondingly, and then the roof will collapse harder. Conversely, the smaller the tension strength  $\sigma_t$  is, the easier the collapse of the overlying strata will be. However, there are more or less soluble components in each stratum. Under the immersion of brine, the solution of the soluble components will lead to the reduction of the tension strength of the stratum, which finally enlarged the collapse possibility.

As regards the protection, a certain thickness of salt formations above the salt cavity should not be mined to prevent the dissolution upward. Especially, for a rock salt protection in the shape of plate in Dongxing Salt Mine, the thickness should be more than 30 m according to the above calculation model, if the tensile strength of integral rock salt is 6 MPa and the Poisson ratio is 0.40. However, the real lower surface of the salt protection is not a plane but an arch, which can greatly enhance its own stability. Therefore, the actual thickness of the salt protection needed is much thinner than 30 m. Besides, specific issues still need to be specifically analyzed because the limit breaking distance is not only related to the mechanical properties of the rock but also related to the dimensions, the buried depth, and the force status.

As further assistance in preventing any undesirable upward solution of the salt formation, an oil pad or blanket should be introduced and maintained to float on top of the brine throughout the operation. For this purpose, oil can be simply added in proper proportion to the solvating liquid as the latter is furnished.

3. As the Poisson ratio  $\mu$  increases, the span criterion  $l_m$  will increase gradually. Considering that the Poisson ratio  $\mu$  only changes in a small range, its influence on the span criterion is not so obvious as the thickness  $h$  and the tension strength  $\sigma_t$ .

In addition, combined with Eqs. (9) and (3), if the buried depth  $H$  is larger, the span criterion  $l_m$  will be smaller conversely. It means that the deeper the immediate roof is buried, the easier it collapses. In another way, to keep it more stable, the roof should be buried not too deep. However, the real collapsed Salt Mines are mostly buried above 600 m, such as Dongxing Salt Mine (400–600 m) (Qiu 2011), Huichang Salt Mine (500 m) (Long and Lin 2011), and Yingcheng Salt Mine (500 m) (Yu 1998a, b). That is, the surface collapse incidents might not occur when the salt caverns are buried deep enough, which will be discussed in the following text.

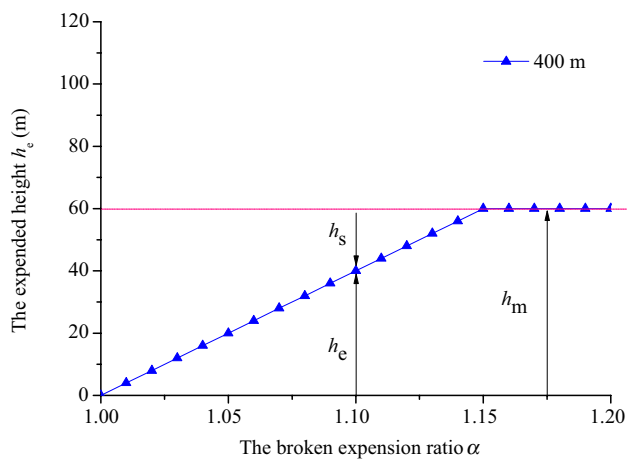


**Fig. 16** Relationship between the broken expansion ratio  $\alpha$  and the expanded height  $h_e$

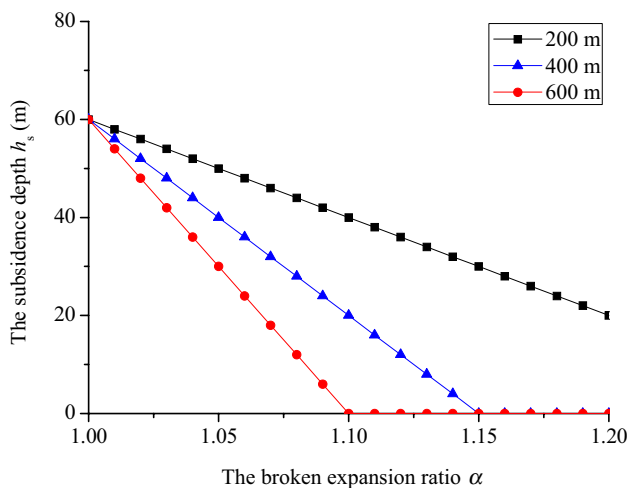


**Fig. 17** Relationship between the broken expansion ratio  $\alpha$  and the subsidence height  $h_s$

**The buried depth**

In fact, after collapsing, the crushing overlying strata will occupy a larger volume than their original. If the whole overlying strata collapse, the final surface subsidence depth  $h_s$  can be simply calculated as follows:

$$h_s = h_m - h_e = h_m - (\alpha - 1) \cdot H, \quad h_s \geq 0, \tag{16}$$

where  $h_s$  indicates the final subsidence depth, m;  $h_m$  indicates the height of a salt cavern or the mining height, m;  $h_e$  indicates the expanded height of the collapsed overlying strata, m;  $\alpha$  indicates the broken expansion ratio, which is the final height of the expanded strata with unit thickness after broken, by supposing that the broken strata are limited in horizontal direction but free in the vertical; and  $H$  is the

buried depth of the salt cavern, namely the thickness of the overlying strata, m.

Supposing that the buried depth  $H$  is 400 m and the mining depth is 60 m, the relationship between the broken expansion ratio  $\alpha$  and the expanded thickness  $h_e$  is shown in Fig. 16. From the figure, as the broken expansion ratio  $\alpha$  increases, the expanded height of the collapsed overlying strata  $h_e$  increases until it reaches the mining height  $h_m$ . Correspondingly, the subsidence depth  $h_s$  becomes smaller.

Supposing that the mining depth is 60 m and the thicknesses of overlying strata are 200, 400 and 600 m, respectively, the relationships between the broken expansion ratio  $\alpha$  and the subsidence height  $h_s$  are shown in Fig. 17. From the figure, the larger the broken expansion ratio  $\alpha$  is, the smaller the subsidence height  $h_s$  will be. Under the same broken expansion ratio  $\alpha$  and the same mining depth, it can be inferred that (1) if the buried depth  $H$  is shallower, the subsidence height  $h_s$  will be larger, namely the collapse of the overlying strata will develop more easily toward the ground surface and form a surface sinkhole; (2) conversely, if the buried depth  $H$  is deeper, the broken part of the overlying strata will find it harder to develop toward the ground surface. In addition, if the broken expansion ratio  $\alpha$  is 1.1 and the buried depth  $H$  is 600 m, the expanded depth  $h_e$  of the overlying strata will be 60 m when the whole overlying strata collapse. In view that the mining height  $h_m$  is also 60 m, the expanded height  $h_e$  is just equal to the height of salt cavern  $h_m$ . In this condition, no surface collapse will occur.

Therefore, considering the bulking effect of the overlying strata, the collapse depth  $h_s$  will not increase linearly with the buried depth  $H$ . If the buried depth is rather deeper, the collapse would have stopped before it develops towards the surface. It succeeds to explain why most of the surface collapse happened above 600 m.

**Conclusion**

In salt mining, the unreasonable salt caverns formed may lead to surface subsidence disasters; it is an urgent technical problem to forecast and even control the collapse of the overlying strata to avoid the surface subsidence. In this paper, a mathematical model was proposed to analyze the collapse mechanism of the overlying strata above a salt cavern by double-well convection. In the proposed model, the collapse of overlying strata was supposed to occur layer by layer, and a thin plate with four edges clamped was introduced to calculate the critical collapse span of each layer. A span criterion  $l_m$  was introduced to distinguish the limit breaking distance. As a case study, the surface collapses at Dongxing Salt Mine were analyzed by the proposed model. Using the proposed model, discussions

were also carried out to study the influence factors of the collapse. Some conclusions are drawn as follows:

1. The limit breaking distance of the thin plate  $b$  is related to the dimensions (the length  $a$  and the thickness  $h$ ), the mechanical properties of the rock (the tension strength  $\sigma_t$  and the Poisson ratio  $\mu$ ), the buried depth ( $H$ , which affects the distributed load  $q$ ) and the force status (the distributed load  $q$ ). To keep the immediate roof more stable, the span criterion  $l_m$  should be larger. In addition, the well spacing should not be too large to maintain the stability of the roof.
2. According to the geophysical exploration, the whole collapse of Dongxing Salt Mine should have happened step by step, namely the overlying strata should be dropped down layer by layer. Once the lowest stratum collapses, the secondary lowest stratum would become the immediate roof of the time and then be suffered from the risk of collapse. By model solution and case study, the surface collapse at Dongxing Salt Mine was verified to be inevitable under its mining and geological conditions. As a protection, a certain thickness of salt formations should be kept above the salt cavity to prevent the dissolution upward. In addition, oil pad or blanket method should be adopted throughout the operation.
3. From the proposed model, the collapse of the overlying strata will happen more easily with the decrease of the thickness, tension strength, and Poisson ratio of each stratum. However, considering the bulking effect of the overlying strata, the collapse depth will not increase linearly with the buried depth. If the buried depth is rather deeper, the collapse would have stopped before it develops to the surface. It succeeds to explain why most of the surface subsidence happened above 600 m.

The above analyses were carried out without considering the regional/local fractures. As a matter of fact, there may be some primary fractures in the strata. The fractures may have an influence on the limit breaking distance in two ways: diminution of the rock mass integrity and changing the mechanical properties. However, it is difficult to obtain the exact distributions and dimensions of these fractures, which makes it hard to quantitatively research the weakness effect of these primary fractures on the strata at present. Therefore, an inadequacy of this study is that the influence of the primary fractures was not considered.

**Acknowledgements** This work was supported by the financial support from National Natural Science Foundation of China (Grant numbers: 51504243, 41877277 and 51674247), the Natural Science Foundation of Jiangsu Province (Grant number: BK20150191), and the Fundamental Research Funds for the Central Universities (Grant number: 2015XKZD06). We are grateful to the anonymous reviewers

and editors for their constructive comments that greatly improved this manuscript.

## References

- Bauer S, Ehgartner B, Levin B, Linn JK (1998) Waste disposal in horizontal solution mined caverns considerations of site location, cavern stability, and development considerations. In: Proceedings of SMRI fall meeting, August 4, 1998, Roma, Italy
- Bekendam R, Paar W (2002) Induction of subsidence by brine removal. In: Proceedings of SMRI fall meeting, October 6–9, 2002, Bad Ischl, Austria
- Bérest P (2016) Craters above salt caverns. In: Proceedings of SMRI spring meeting, April 25–26, 2016, Texas, USA
- Buffet A (1998) The collapse of Compagnie des Salins SG4 and SG5 drillings. In: Proceedings of SMRI fall meeting, August 4, 1998, Rome, Italy
- Cai MF, He MC, Liu DY (2002) Rock mechanics and engineering. Science Press, Beijing
- Contrucci I, Klein E, Cao NT, Daupley X, Bigarré P (2011) Multi-parameter monitoring of a solution mining cavern collapse: first insight of precursors. *CR Geosci* 343(1):1–10
- Dahm T, Heimann S, Bialowons W (2011) A seismological study of shallow weak earthquakes in the urban area of Hamburg city, Germany, and its possible relation to salt dissolution. *Nat Hazards* 58(5):1111–1134
- Fan YQ, Li XF (2008) Study of 3D finite-element modeling on the law of solution mining subsidence. *Ind Miner Proces* 9:22–24 + 29
- Ge HX, Jackson MPA (1998) Physical modeling of structures formed by salt withdrawal: implications for deformation caused by salt dissolution. *AAPG Bulletin* 82(2):228–250
- Gutierrez F, Parise M, De Waele J, Jourde H (2014) A review on natural and human-induced geohazards and impacts in karst. *Earth-Sci Rev* 138:61–88
- Gutiérrez F, Guerrero J, Lucha P (2008) A genetic classification of sinkholes illustrated from evaporate paleokarst exposures in Spain. *Environ Geol* 53(5):993–1006
- Iovine G, Parise M (2008) I sinkholes in Calabria. *Memorie Descrittive della Carta Geologica d'Italia* 85:335–386
- Jeanneau V (2005) The sinkhole of the cavity LR 50/51 in La Rape Area, a case history. RHODIA Company. In: Proceedings of SMRI Fall Meeting, October 2–5, 2005, Nancy, France
- Jiang DY, Ren S, Liu XR, Liu BX (2005) Stability analysis of rock salt cavern with catastrophe theory. *Rock Soil Mech* 26(7):1099–1103
- Johnson KS (1998) Land subsidence above man-made salt-dissolution cavities. In: Borchers JW (ed) Land subsidence case studies and current research: proceedings of the Dr. Joseph F. Poland symposium on land subsidence. *Assoc Eng Geol Spec Publ* vol 8, pp. 385–392
- Johnson KS (2005) Subsidence hazards due to evaporates dissolution in the United States. *Environ Geol* 48:395–409
- Johnson KS (2008) Evaporate-karst problems and studies in the USA. *Environ Geol* 53:937–943
- Karimi-Jafari M, Bérest P, Brouard B (2008) Subsidence, sinkholes and craters above salt caverns. In: Proceedings of SMRI spring meeting, April 28–29, 2008, Porto, Portuguesa
- Li XF, Tang SH, Fan YQ (2008) Study on ground subsidence mechanism of solution mining and control measure. *Ind Miner Proces* 11:27–29 + 44
- Li XF, Xu BG, Tang SH (2009) Research on ground subsidence mechanism of solution mining by drilling and control measure. *J Saf Sci Technol* 5(1):131–134

- Li YP, Liu W, Yang CH, Daemen JJK (2014) Experimental investigation of mechanical behavior of bedded rock salt containing inclined interlayer. *Int J Rock Mech Min Sci* 69:39–49
- Liu XR, Jiang DY, Tan XH (1999) The study of settlement and deformation law of the dissolutions overlying strata in solution mining. *Ind Miner Proces* 17(7):23–27
- Liu BX, Jiang DY, Liu XR (2007) Analysis and control on roof stability of rock-salt cavity. *J Chongqing Univ (Nat Sci Edit)* 30(3):133–135
- Liu HL, Yang TH, Zhang PH, Li Y, Qin T, Yu QL (2015) “OX” failure pattern of roof and strata-pressure behavior under complex geological conditions. *J Min Saf Eng* 32(5):793–800
- Long HR, Lin ZS (2011) Surface sinkhole of Jiangxi Huichang is to salt mining. Chinese land resources report. [http://www.mlr.gov.cn/kczygl/ksdzjh/201101/t20110106\\_809977.htm](http://www.mlr.gov.cn/kczygl/ksdzjh/201101/t20110106_809977.htm). Accessed 22 Aug 2018
- Mancini F, Stecchi F, Zanni M, Gabbianelli G (2009) Monitoring ground subsidence induced by salt mining in the city of Tuzla (Bosnia & Herzegovina). *Environ Geol* 58:381–389
- Mesescu AA (2011) The Ocnele Mari salt mine collapsing sinkhole. A NATECH breakdown in the Romanian Sub-Carpathians. *Carpathian J Earth Environ Sci* 6(1):215–220
- Michael SB, Maurice BD (2002) Geomechanical analysis of pressure limits for thin bedded salt caverns. In: Proceedings of SMRI spring meeting, April 29–30, 2002, Banff, Canada
- Parise M (2015) A procedure for evaluating the susceptibility to natural and anthropogenic sinkholes. *Georisk* 9(4):272–285
- Parise M, Lollino P (2011) A preliminary analysis of failure mechanisms in karst and man-made underground caves in southern Italy. *Geomorphology* 134(1–2):132–143
- Poppe S, Holohan EP, Pauwels E, Cnudde V, Matthieu Kervyn M (2014) Sinkholes, pit craters, and small calderas: analog models of depletion-induced collapse analyzed by computed X-ray microtomography. *Geol Soc Am Bull* 127(1–2):281–296
- Qian MG, He FL (1991) Behaviour of the main roof in longwall mining—weighting span, fracture and disturbance. *Int J Rock Mech Min Sci* 28(1):A53
- Qian MG, Xu JL (1998) Study on the “O-Shape” circle distribution characteristics of mining-induced fractures in the overlying strata. *J China Coal Soc* 23(5):466–469
- Qian MG, Shi PW, Xu JL (2010) Mining pressure and strata control. China University of Mining and Technology Press, Xuzhou
- Qiu ZY (2011) Mechanism analysis of surface collapse in the area of solution salt mining. *J Saf Sci Technol* 7(12):27–31
- Ren S (2005) Study on the mechanism and the prediction model of the subsidence caused by rock salt solution mining. Ph.D. thesis, Chongqing University, Chongqing, China
- Ren S, Jiang DY, Yang CH, Jiang ZW (2007) Study on a new probability integral 3D model for forecasting solution mining subsidence of rock salt. *Rock Soil Mech* 28(1):133–138
- Ren S, Jiang DY, Yang CH (2009) Stratification transfer model for predicting complex mining subsidence. *J Chongqing Univ* 32(7):823–828
- Shi XL, Li YP, Yang CH, Xu YL, Ma HL, Liu W, Ji GD (2015) Influences of filling abandoned salt caverns with alkali wastes on surface subsidence. *Environ Earth Sci* 73:6939–6950
- Ulusay R (2014) The ISRM suggested methods for rock characterization, testing and monitoring: 2007–2014. Springer, Netherlands
- Vigna B, Fiorucci A, Banzato C, Forti P, De Waele J (2010) Hypogene gypsum karst and sinkhole formation at Moncalvo (Asti, Italy). *Z Geomorphol* 54(S2):285–308
- Waltham T, Bell F, Culshaw M (2005) Sinkholes and subsidence. Springer, Netherlands
- Wang ZT, Qian MG (1989) The calculating methods of the first weighting span of main roof. *J China Univ Min Tech* 18(2):9–18
- Yu YJ (1998a) Research on the cavern and analysis on the surface subsidence in thin layered salt formation by solution mining (I). *China Well Rock Salt* 29(2):14–17
- Yu YJ (1998b) Research on the cavern and analysis on the surface subsidence in thin layered salt formation by solution mining (II). *China Well Rock Salt* 29(3):12–17
- Zhang K, Wang QS (2010) The shallow seismic reflection survey in the prediction of the collapse. *Geophys Geochem Explor* 34(1):85–88
- Zhang GM, Li YP, Yang CH, Daemen JJK (2014) Stability and tightness evaluation of bedded rock salt formations for underground gas/oil storage. *Acta Geotech* 9(1):161–179
- Zhang GM, Li YP, Daemen JJK, Yang CH, Wu Y, Zhang K, Chen YL (2015a) Geotechnical feasibility analysis of compressed air energy storage (CAES) in bedded salt formations in Huai’an city, China. *Rock Mech Rock Eng* 48(5):2111–2127
- Zhang GM, Wu Y, Wang LJ, Zhang K, Daemen JJK, Liu W (2015b) Time-dependent subsidence prediction model and influence factor analysis for underground gas storages in bedded salt formations. *Eng Geol* 187:156–169
- Zhang K, Wang QS, Huang SH, Zhang X (2015c) Research on the collapse mechanism and its monitoring and prediction technology in Dingyuan Salt Mine. In: Proceedings of 2015 academic conference of geophysical technology, March 20, 2015, Hefei, China
- Zhang GM, Wang LJ, Wu Y, Li YP, Yu SY (2017) Failure mechanism of bedded salt formations surrounding salt caverns for underground gas storage. *Bull Eng Geol Environ* 76(4):1609–1625